Power Sharing and Voltage Regulation in Islanded DC Microgrids with Centralized Double-Layer Hierarchical Control

Yuan Yao
School of Electrical & Electronic Engineering
The University of Adelaide
Adelaide, Australia
yuan.yao@adelaide.edu.au

Nesimi Ertugrul
School of Electrical & Electronic Engineering
The University of Adelaide
Adelaide, Australia
nesimi.ertugrul@adelaide.edu.au

Ali Pourmousavi Kani
School of Electrical & Electronic Engineering
The University of Adelaide
Adelaide, Australia
a.pourm@adelaide.edu.au

***Abstract*—As the conventional AC power grid is evolving with the integration of renewable energy resources (PV and wind) and power electronic converters, we discover more technical and economic values for DC microgrids (MGs), particularly with electric vehicles (EVs) and battery energy storage systems (BESSs) changing the load landscape. This paper presents a double-layer centralized hierarchical control framework to achieve the DC bus voltage regulation and power coordination of a PV-BESSs based DC MG, which operates in fully islanding condition. The proposed control strategy consists of two levels: 1) The primary control can achieve the DC bus voltage regulation by modifying the commonly-used inner and outer PI control loops; 2) The secondary control considers the characteristics of different types of BESSs. The latter is also responsible for load sharing by generating power/current reference signals among different DGs and DC converters. The advantage of the proposed control strategy is to eliminate the droop control as well as the conventional secondary control, which is designed to restore the voltage deviation caused by droop equations in a three-level hierarchical control system. The simulation results show that the proposed control strategy is effective to stabilize the DC bus voltage and it can share the dynamic power variation within DC MG.**

Keywords—DC microgrid, hierarchical control, distributed generation, DC-DC converter, power coordination, voltage regulation

I. INTRODUCTION

The exponential growth of solar, wind and battery technologies are changing the power grid as we know today, exacerbated by the changes in behind-the-meter load demand and distributed energy resources. Some of the major issues during the grid transformation are diminishing power quality, reduced reliability and high energy cost. To address the issues as well as to respond to rapid climate change and severe environmental consequences, the idea of microgrids (MGs) with predominantly renewable generation emerged as a prominent solution [1]. MGs are ideal platforms to integrate distributed generators (DGs), renewable energy resources (RESs), as a subset of the macro grid and fringe of grids and various emerging load types including EVs and battery storage systems.

Although the existing infrastructure of power network still favours AC MGs, DC MGs can offer various unique and unparalleled benefits compared to AC systems [2], [3]. For example, the challenges with synchronization, difficulties in reactive power management and excessive transmission and distribution level bidirectional losses, reduction in power system inertia, and power quality issues can be relieved in a DC MG. In addition, considering the DC output of common RESs and emerging loads which are primarily DC, the DC distribution system and DC MGs is likely to dominate the grid transformation towards a smarter grid . The emerging research in power electronics and wide-bandgap devices also implies a shift towards DC paradigm [2]-[4].

Increasing penetration of solar photovoltaic (PV) sources at residential and community level raises concerns regarding reverse power flow at both the distribution and the transmission networks. This alters the way of designing and constructing the future power network. On the other hand, solar PV (and wind power) has inherent intermittency in generation. MGs can address this issue in a more efficient way by conveniently integrating a battery energy storage system (BESS), which is DC. Although the relatively high cost and low lifespan of the existing BESS limit the battery uptake at the household level, MG level integration as community storage is an economically sound solution for consumers. Further advancements in battery chemistry and the cost reduction will play a significant role in shaping the structure of future MGs.

The coordination and control of DC MGs mainly applies to power-electronics converters. Wide utilization of these converters provides flexibility in power flow management and ease of control, especially current-sharing among MGs. In PV-BESS based DC MGs, boost converters and bidirectional DC-DC converters are widely used (see Fig. 1). A common DC voltage bus is necessary in DC MGs to interconnect power converters together and meet the load demand. This bus is connected to the external power grid via a high-power bidirectional DC-DC converter for a DC grid or to an AC grid via a bidirectional inverter. If the MG is connected to an external grid, the DC bus voltage within the DC MG will be determined by the grid voltage. However, one of the crucial objectives of a MG is to operate without any support from the external power grid, which is also known as islanded mode operation. Therefore, MGs should be capable of forming and maintaining the DC bus voltage level independent from the external grid.

In most of the hierarchical controlled MGs, the primary control aims at load sharing by adopting the I-V droop control. Although this method performs reasonably well by sensing local output voltage only, it has several inherent disadvantages such as imposing voltage deviation, ignoring the dynamics of loads and poor transient performance of power sharing due to fixed droop coefficients [5]-[7].

978-1-6654-3451-5/21/$31.00 ©2021 IEEE

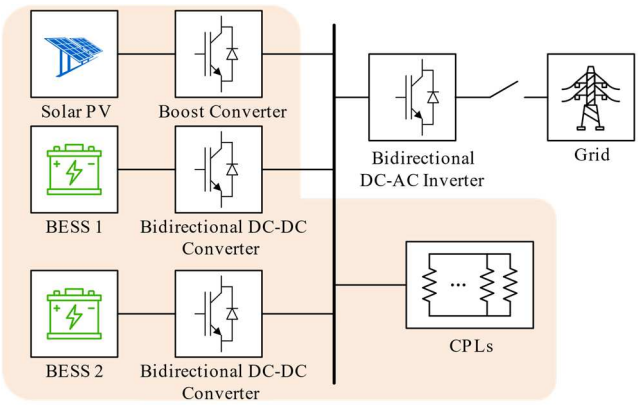

Fig. 1. A hypothetical configuration of a DC MG with solar PV, two BESSs and loads.

To address these issues, this paper proposes a centralized two-level hierarchical control strategy for a small-scale PV-BESS DC MG. The main contributions are concluded as: 1) Utilizing the distributed non-droop-based voltage and current control loops as primary control which simplifies the design complexity of primary control as well as reducing the communication aspects. 2) The centralized decision-making secondary control enables either solar system or BESSs to establish the bus voltage level under fully islanded condition by dispatching the desired power output signals to each DG. This proposed supervisory control not only guarantees the ability of DC MG operating modes transition, but also ensures full use of renewable generation when possible.

The paper is organized as follows: The structure and modelling of the DC MG is presented in Section II. Section III details the configuration and design of the hierarchical control strategy for power coordination and voltage restoration. Section IV shows the simulation results using the models developed and control framework defined in the previous sections.

II. DC MICROGRIDS TOPOLOGY AND MODELS

The overall layout of the DC MG studied in this paper is shown in Fig. 1. Note that this small-scale DC MG (aimed to be used in a household) consists of a 6.2 kW solar system, a lithium-ion BESS, a lead-acid BESS and DC loads, which has been modelled. A common DC bus with nominal voltage of 400 V DC is selected to connect them together to form the DC MG. The DC loads are attached to the DC bus via buck converters and assumed to behave as constant power loads (CPLs). By controlling the buck converters, the load voltages can be maintained at their rated value.

Note that, the CPLs and their corresponding buck converters are considered in a single block to reduce the complexity, in which the CPLs have a maximum demand of 12 kW. Moreover, as the DC MG topology discussed in this paper can be viewed as a typical residential application, both DGs and loads are located close to each other. Thus, the line impedance within DC MG can be neglected.

The solar panel used in this paper consists of 3 strings in parallel, where each string has 9 series-connected PV modules. A DC-DC boost converter is employed to enable the PV system operating in two modes: 1) Maximum power point tracking (MPPT), and 2) DC bus voltage control. The MPPT controller monitors the solar panel output voltage and current to generate a reference voltage signal by using the perturb and observe (P&O) approach [8]. In the absence of external grid to form the voltage for the MG (i.e. BESSs are charging and no grid connection), the solar boost converter is controlled as a voltage source, which can regulate the bus voltage within a given range.

As shown in Fig. 1, there are two BESSs in this DC MG, which are connected with a bidirectional DC-DC converter to allow charging and discharging operation of the BESSs. The first BESS is assumed to be a lithium-ion battery with 50 V

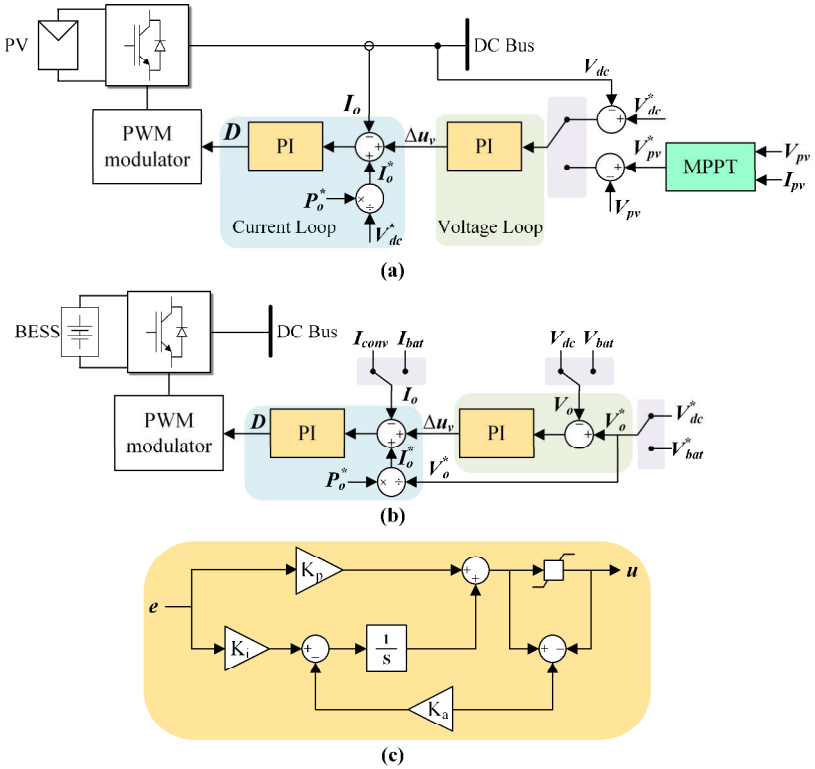

Fig. 2. The primary control strategy of a) PV, b) BESS and c) PI controller block diagram with back-calculation anti-windup.

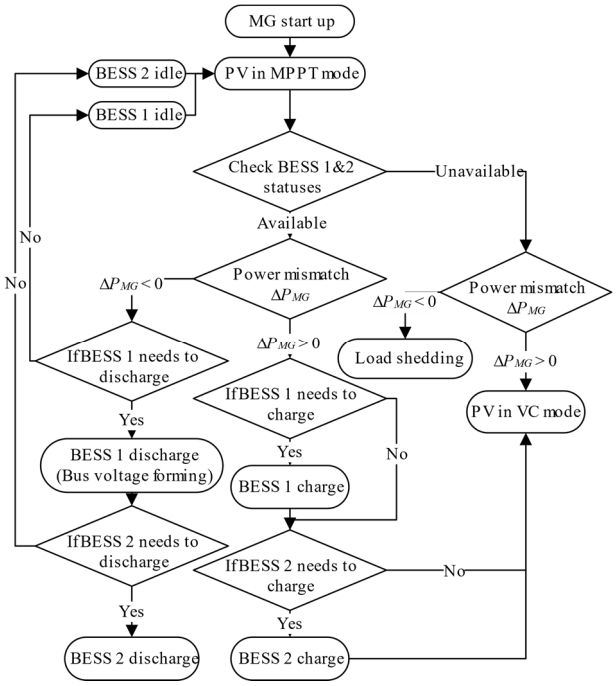

Fig. 3. The proposed centralized secondary control structure.

nominal voltage and 50 Ah capacity. The second BESS utilizes the conventional lead-acid battery as a back-up storage. The lithium-ion battery usually has longer lifecycle, higher energy density and faster response time compared to the lead-acid batteries [9]. Therefore, the proposed control strategy considers these contrasting characteristics by prioritising BESS 1 as the primary storage in the MG. Therefore, BESS 2 only operates when BESS 1 cannot provide sufficient power or when it is unavailable. The details of the BESSs control algorithm will be discussed in the next section.

III. Centralized hierarchical control stratrgy for DC-DC converters

The proposed hierarchical control structure is shown in Fig. 2. It illustrates the overall framework of the proposed hierarchical control where each DG or DER has a distributed primary control while being orchestrated by a centralized secondary (supervisory) control system. For small-scale DC MG applications, the number of DGs and DERs are small and these energy sources are usually close to the loads. Therefore, a centralized hierarchical structure can reduce the complexity of control system at the generation side, and improve the total control system efficiency compared with the fully distributed control.

A. The primary control

One of the most common topologies for the primary control is double PI-based loops where the outer loop regulates the converter output voltage and inner loop adjusts the inductor current. As it was mentioned in the introduction, the traditional droop method only relies on the voltage loop to generate the current refence values for inner loop which compromises the accuracy of voltage regulation. Thus, an additional layer of PI control is desired to restore this voltage error in the conventional hierarchical control system [3]. The presented primary control in this paper introduces an individual current reference from the secondary supervisory control. As a result, the outer voltage loop is not responsible for providing the current reference value for the inner loop. Therefore, the additional layer of PI controller for voltage correction can be eliminated.

Figs. 2(a) and 2(b) present the proposed primary control strategy for the solar PV and the BESS. This primary control is implemented in a distributed way to regulate the output power based on the incoming reference signal from the secondary level. It contains two parts: the mode (refence signals) selection and voltage and current control loops. For mode selection, the configuration of this part varies from source to source. The solar PV can be controlled in either MPPT mode or voltage control (VC) mode, where the BESS is able to charge or discharge following the command sent from the secondary controller.

In the context of local converter control, the outer loop receives the reference voltage signal from the mode switch and generates the correcting value to stabilize the bus voltage. The inner current loop obtains its reference value from the secondary controller as well as the voltage compensation signal from the outer loop. Hence, this strategy avoids the use of droop equations and decouples the voltage controller from the inner current loop, meaning that the converter current/power can be easily coordinated without imposing the output voltage fluctuation. Moreover, the anti-windup back-calculation method [10] is carried out to provide extra flexibility on PI controller gains tunning as demonstrated in Fig. 2(c).

B. The secondary (supervisory) controller

The proposed secondary controller is designed to monitor the power mismatch ($\Delta P_{MG} = P_{PV} - P_{Load}$) between solar PV and loads to determine the associated power reference signals for the two BESSs, where P_{PV} is the output power from the solar panel and P_{Load} is the total demand of the DC loads. Also, this mismatch signal is used to identify the desired operating modes for PV and BESSs. A flowchart with the detailed decision-making process of the proposed power management strategy has been shown in Fig. 3.

During the start-up stage of the DC MG, solar PV is set to MPPT mode by default. Then the availability of BESSs are checked before generating reference output power signals for the BESSs. If all BESSs can charge or discharge, the power mismatch is computed. When the PV power is higher than total load demand, $\Delta P_{MG} > 0$, there is excessive power for charging the BESSs. Hence, BESS 1 will be charged first since the lithium-ion battery has better performance in power smoothing compared to lead-acid battery. If it is not sufficient to compensate the power mismatch (e.g., BESS 1 has been fully charged or the charging current exceeds its rated value), then BESS 2 will be charged at the same time. Once both BESSs operate in charging mode, the PV is commanded to switch to voltage regulation mode to stabilize the bus voltage.

On the other hand, if the CPLs require more power than is generated by the solar PV system at MPPT, BESS 1 will discharge first and contribute in forming the bus voltage. When the sum of generated power from PV and BESS 1 is lower than the total demand or the discharging current of BESS 1 reaches the maximum value, the BESS 2 will be activated to share the rest of power consumption. The most extreme condition is when two BESSs are unable to operate. In that case, the PV will switch to voltage control mode if the power mismatch is less than 0. Otherwise, the load shedding operation is necessary to maintain the safe operation of the DC

TABLE I. CONFIGURATION OF THE DC MG PARAMETERS.

Control Parameters	Value	Control Parameters	Value
$K_{p\_V\_PV\_MPPT}$	8	$K_{p\_V\_BESS}$	0.5
$K_{i\_V\_PV\_MPPT}$	47	$K_{i\_V\_BESS}$	2.5
$K_{p\_I\_PV\_MPPT}$	0.6	$K_{p\_I\_BESS}$	0.02
$K_{i\_I\_PV\_MPPT}$	8.9	$K_{i\_I\_BESS}$	25
$K_{p\_V\_PV\_VC}$	0.5	K_{a_PV}, K_{a_BESS}	1
$K_{i\_V\_PV\_VC}$	15	f_{conv_PV}	5 kHz
$K_{p\_I\_PV\_VC}$	0.2	f_{conv_BESS}	10 kHz
$K_{i\_I\_PV\_VC}$	8	$f_{control}$	2 kHz

MG. Some advantages of the proposed supervisory control strategy are: 1) making full use of the solar power by maximizing the possibility of MPPT operation, 2) extending the battery storage life by operating the BESS based on their capabilities, and 3) reducing the complexity of the local controller design due to the centralized topology.

IV. SIMULATION RESULTS

The DC MG model and proposed hierarchical control system for power coordination are implemented and analysed using MATLAB/Simulink. Different simulation scenarios have been performed to investigate the performance of the proposed hierarchical control framework under normal operation of the DC MG with variations in load demand, weather impact on PV generation, and the charging and discharging of BESSs. Table I summarizes the control parameters defined and corresponding values used in the hierarchical control system.

A. *Case 1: Step Load*

In this case, the impact of load demand changes are investigated by applying various step load changes in 0.5 s intervals. The solar PV is assumed to operate at constant solar irradiance of 1000 W/m^2 at cell temperature of 25 °C.

Fig. 4 shows the DC bus voltage and load demand variation as well as power output from PV and BESSs during this simulation case. The DC MG starts with a 12 kW load demand from t = 0 to 0.5 s, the PV is maintained at maximum power of 6.2 kW by MPPT controller. The BESS 1 begins to discharge at its maximum current/power and establish the bus voltage. However, there is still a power imbalance around 2 kW. Hence, the BESS 2 is switched on by the secondary control to meet this power demand. At t = 0.5 s, the total load drops to 8 kW and the power mismatch at this moment is lower than BESS 1 discharging limit. Thus, the BESS 2 shuts down while the PV still remains in MPPT mode. At t = 1 s, another 4-kW load disconnects and the power mismatch ΔP_{MG} becomes greater than 0 kW. Consequently, the extra 2 kW power generation is flowing into BESS 1 to store the excessive energy. In the meantime, the PV voltage control mode is activated as there is no BESS discharging to support the bus voltage level. From t = 1.5 to 2 s, the load decreases further to 2 kW. This sudden change results the BESS 1 being charged at maximum power rate, i.e., 2 kW. Since the PV output power is higher than the sum of the load and BESS 1 charging power limit, BESS 2 starts to charge to achieve power balance.

After t = 2 s, the total load demand goes back to 12 kW at the same rate as of the decreasing period. Because the load is still lower than the maximum PV power , the PV system is kept operating at voltage regulation mode while BESS 1 contributes to power sharing. From t = 2.5 to 3 s, the PV resumes its MPPT tracking mode with an 8 kW demand in the grid. However, the speed of MPPT tracking is slower than the rate of change in load power. Hence, the PV output power gradually approaches to maximum value while BESS 1 and 2 discharge to compensate the extra demand. The maximum bus voltage fluctuation in this case is about 3 V, which indicates no more than 1% of voltage ripple on the DC bus under the

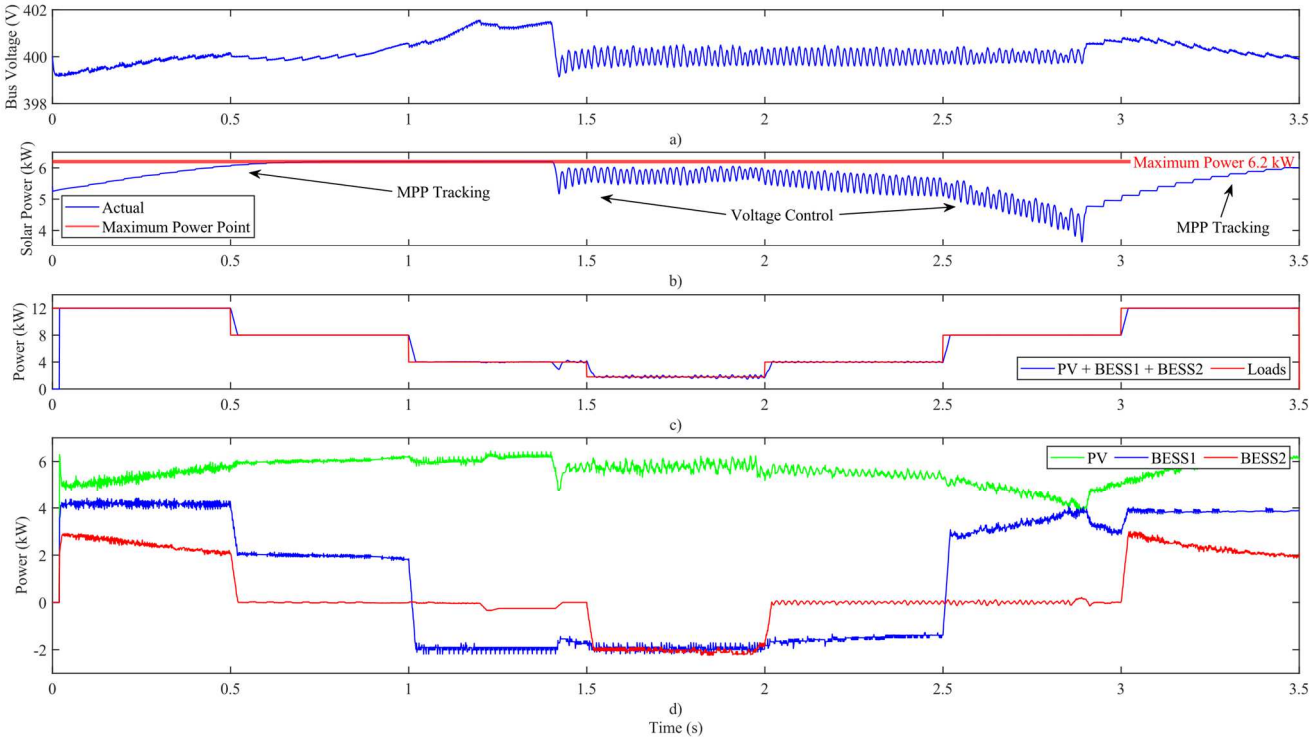

Fig. 4. Case 1: a) DC bus voltage, b) solar power and MPPT, c) power of DERs and load, d) power of PV and BESSs.

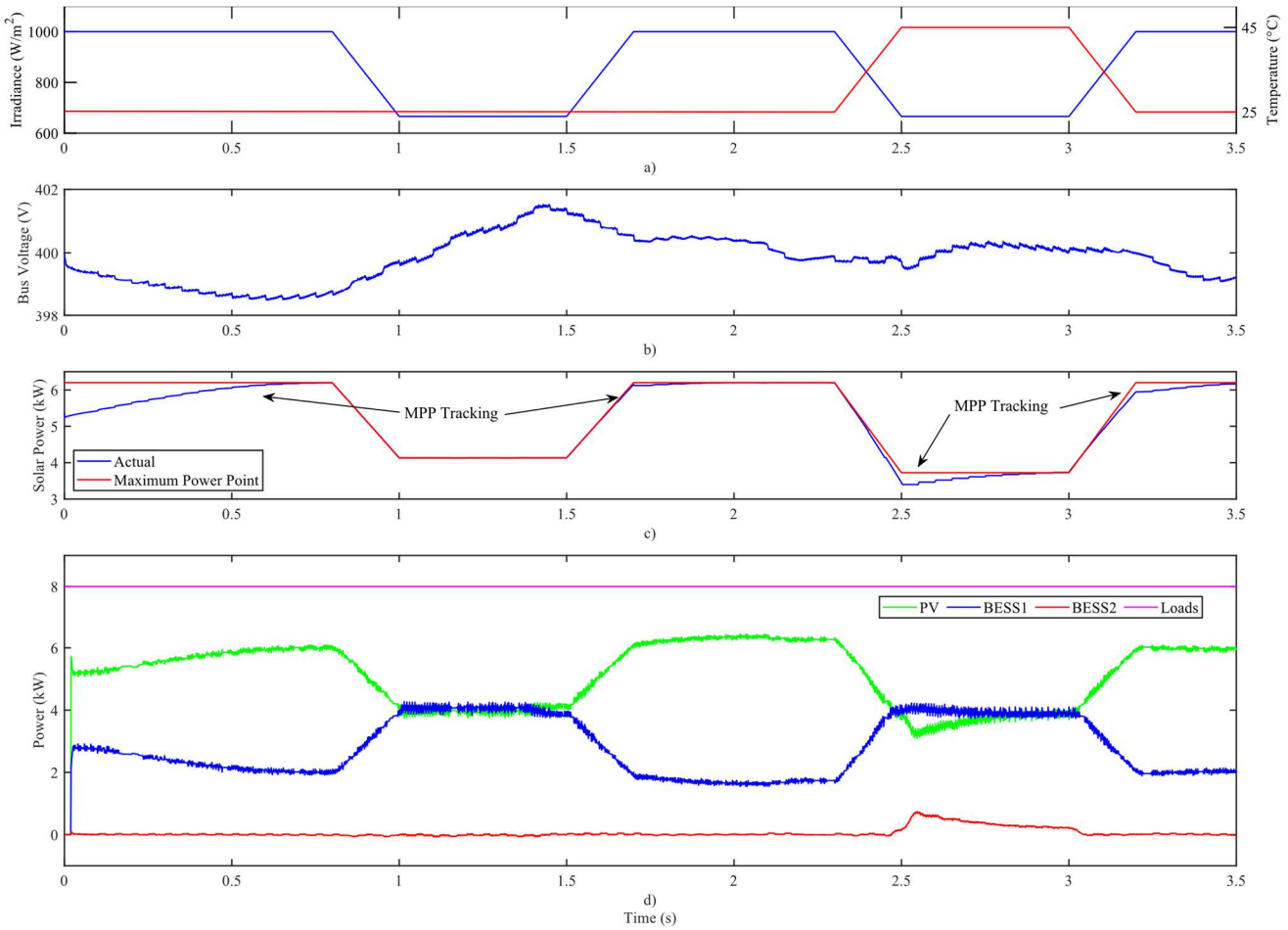

Fig. 5. Case 2: a) solar irradiance and temperature, b) DC bus voltage, c) solar power and MPPT, d) power of PV, BESSs and loads.

load change scenarios, and the total load demand is fulfilled the whole time, as shown in Fig. 4(c).

B. *Case 2: Solar Irradiance and Temperature Variations*

In this case, the demand of CPLs is maintained at 8 kW, while the weather-related factors are varied to justify the performance of the proposed hierarchical controller. Ramp-up and ramp-down variations are observed for both the solar irradiance and the cell temperature, as shown in Fig. 5(a). It can be seen in Fig. 5(c) that reduction in solar irradiance and rising in cell temperature lead to a reduction in PV generation. However, the pattern of these variations is different from each other as the change in PV power has a linear relationship with irradiance while the cell temperature alteration produces a nonlinear shift in output power.

Fig. 5(d) shows the power sharing among PV and BESSs with the constant load demand. BESS 1 compensates the power reduction due to these variations. From t = 0.5 to 2 s, since the maximum power mismatch is less than 4 kW which is the discharging limit of BESS 1, BESS 2 remains idle during the whole this interval. However, from t = 2 to 3.5 s, the PV output power can drop below 4 kW due to the cell temperature increment. Then, BESS 2 is instructed to discharge at t = 2.5 s in order to compensate this power mismatch. Fig. 5(b) implies that the bus voltage is well regulated at 400 V with the largest fluctuation to be around 0.75%.

C. *Case 3:Combined Test*

In the final case, the load variations described in Case 1 and weather-related changes from Case 2 are combined together to verify the operational response of the DC MG with the proposed hierarchical control strategy under practical scenario. The same load step changes used in Case 1 (Fig. 4c) as well as the ramp-up and -down fluctuations of solar irradiance and cell temperature (Fig. 5a) are applied to the DC MG simultaneously.

Fig. 6 demonstrates the system operation including bus voltage, output power of solar PV and its maximum power point reference, the load demand and power sharing among the sources. In Fig. 6(a), the bus voltage is stabilized at its nominal value throughout the whole simulation process. As it can be seen from Fig. 6(b), the PV always tracks the maximum power point from t = 0 to 1.5 s and from t = 2.4 to 3.5 s. It only works in voltage regulation mode between t = 1.5 to 2.4 s due to BESS 1 and 2 are charged as the power mismatch is positive ($\Delta P_{MG} > 0$). Moreover, Fig. 6(c) illustrates that the load demand is satisfied all the time no matter how the power of PV and BESSs varied. Fig. 6(d) shows that BESS 1 contributes more than BESS 2 in the power sharing effort according to the design objective, which is to utilize lithium-ion battery as the primary source to smooth the power imbalance between other DERs and loads. The comparison between BESS 1's and 2's actual power output with their desired values are displayed in Fig. 7, which indicates the good capability of the power reference tracking by adopting the proposed primary and secondary control.

V. Conclusion

The proposed hierarchical control strategy is designed to achieve the proper load sharing as well as the regulation of bus

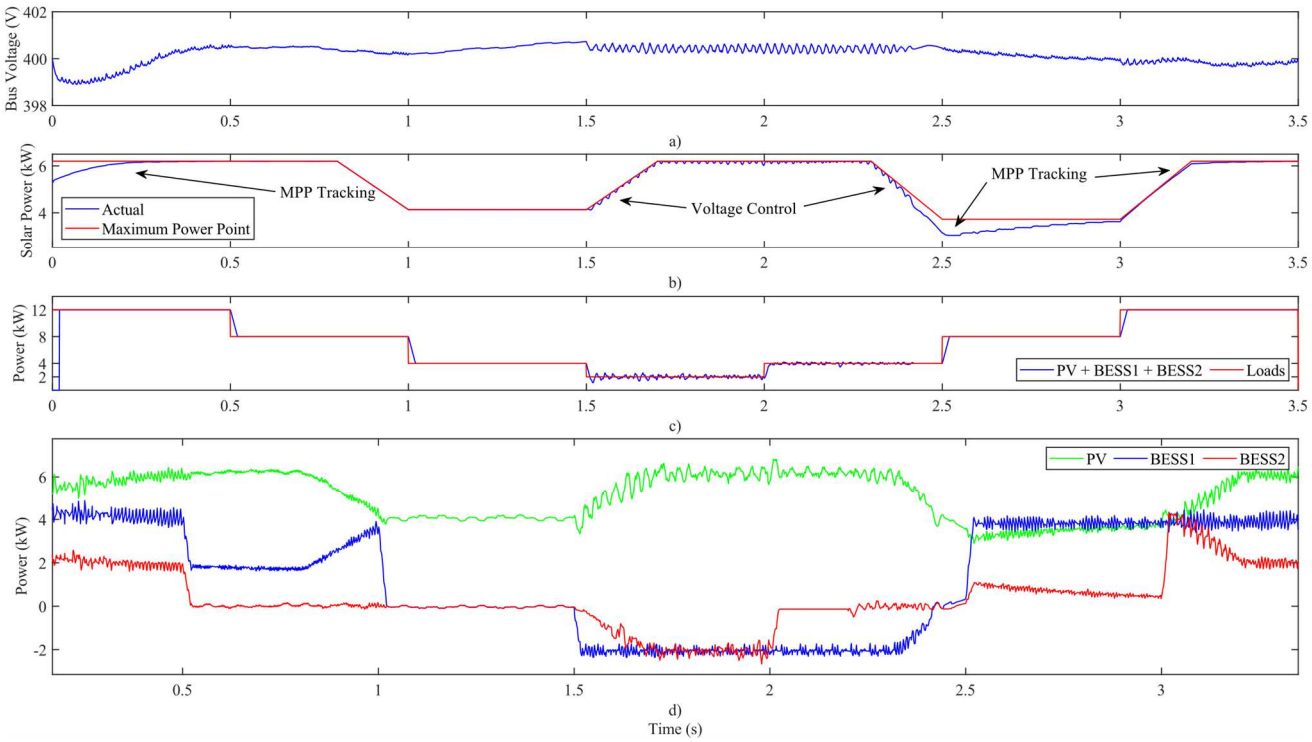

Fig. 6. Case 3: a) DC bus voltage, b) solar power and MPPT, c) power of generations and loads, d) power of PV and BESSs.

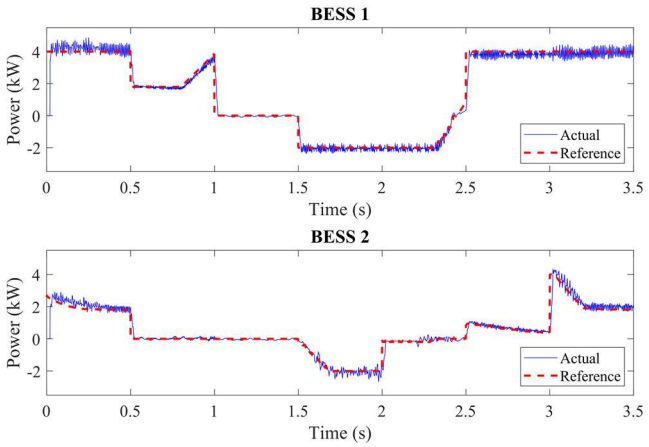

Fig. 7. Power tracking of BESS 1 & 2 in Case 3.

voltage for small-scale DC MGs. This control framework contains distributed local converter controllers with improved voltage and current control loops and a centralized secondary control level for supervising all units within the DC MG to provide output power referencing signals for each component. By employing the proposed method, the conventional droop control for current-sharing can be avoided. Therefore, there is no extra middle layer of voltage restoration control by implementing the proposed hierarchical control structure.

The feasibility and stability of fully islanded operation of DC MG have been investigated and justified under several practical simulation experiments. The simulation results prove that the proposed hierarchical control strategy is effective and ideal to enable the community-level DC MGs' autonomous operation without external grid support. We are planning to test the proposed method in a hardware-in-the-loop (HIL) simulation study with real hardware components and the operation of multiple DC MGs in the future.

REFERENCES

[1] J. M. Guerrero, J. C. Vasquez, J. Matas, L. G. d. Vicuna, and M. Castilla, "Hierarchical Control of Droop-Controlled AC and DC Microgrids—A General Approach Toward Standardization," IEEE Transactions on Industrial Electronics, vol. 58, no. 1, pp. 158-172, 2011.

[2] N. Ertugrul and D. Abbott, "DC is the Future [Point of View]," in Proceedings of the IEEE, vol. 108, no. 5, pp. 615-624, May 2020.

[3] C. Jin, P. Wang, J. Xiao, Y. Tang and F. H. Choo, "Implementation of Hierarchical Control in DC Microgrids," in IEEE Transactions on Industrial Electronics, vol. 61, no. 8, pp. 4032-4042, Aug. 2014.

[4] J. Xiao, P. Wang and L. Setyawan, "Hierarchical Control of Hybrid Energy Storage System in DC Microgrids," in IEEE Transactions on Industrial Electronics, vol. 62, no. 8, pp. 4915-4924, Aug. 2015

[5] O. Palizban, and K. Kauhaniemi, "Hierarchical control structure in microgrids with distributed generation: Island and grid-connected mode," Renewable and Sustainable Energy Reviews, vol. 44, pp. 797-813, April 2015.

[6] Z. Peng, J. Wang, D. Bi, Y. Wen, Y. Dai, X. Yin, and Z. J. Shen, "Droop Control Strategy Incorporating Coupling Compensation and Virtual Impedance for Microgrid Application," IEEE Transactions on Energy Conversion, vol. 34, no. 1, pp. 277-291, March 2019.

[7] Y. Yao and N. Ertugrul, "An Overview of Hierarchical Control Strategies for Microgrids," 2019 29th Australasian Universities Power Engineering Conference (AUPEC), pp. 1-6, 2019.

[8] N. Femia, G. Petrone, G. Spagnuolo and M. Vitelli, "Optimization of perturb and observe maximum power point tracking method," in IEEE Transactions on Power Electronics, vol. 20, no. 4, pp. 963-973, July 2005.

[9] S. Vazquez, S. M. Lukic, E. Galvan, L. G. Franquelo and J. M. Carrasco, "Energy Storage Systems for Transport and Grid Applications," in IEEE Transactions on Industrial Electronics, vol. 57, no. 12, pp. 3881-3895, Dec. 2010.

[10] J. Choi and S. Lee, "Antiwindup Strategy for PI-Type Speed Controller," in IEEE Transactions on Industrial Electronics, vol. 56, no. 6, pp. 2039-2046, June 2009.